COMPUTATION OF AXILAL DIDPERSION AND OVERALL LIQUID-SOLID MASS COEFFIENTS FOR A TRICKLE-BED REACTOR BY USING THE TRACER TECHNIQUE

Jornandes Dias da Silva, e-mail: jornandes.dias@pq.cnpq.br
Polytechnic School, University of Pernambuco-UPE, Rua Benfica - 455, Environmental and Energetic Technology Laboratory, Madalena, Cep: 50750-470, phones: (081) 3184-7529 or (081) 8864-8392, Recife - PE, Brazil.

Abstract. *Experimental evaluation and dynamic modelling were presented for a liquid flow (H_2O + NaOH tracer) on solid particles in trickle beds. A dynamic mathematical model was described to study the gas-liquid-solid process in which the liquid phase together with the NaOH tracer is treated as a continuum. The physical model has been analyzed by using the formulation of initial and boundary conditions and its solution methodology. An experimental procedure to measure the concentrations of the NaOH tracer has been performed. The concentration measurements for the NaOH tracer have been performed in a fixed bed reactor under trickling flow of the liquid phase on the range of operating conditions. The varying parameters are axial dispersion of the liquid phase and overall liquid-solid mass transfer coefficient. Results of the mathematical model were presented and validated. The model has been validated by comparison using two experimental cases. The optimized values of the axial dispersion of the liquid phase ($D_{ax,L}$) and overall liquid-solid mass transfer ($(Ka)_{LS}$) coefficient were obtained simultaneously by using the quadratic objective function. To represent the behavior of $D_{ax,L}$ and $(Ka)_{LS}$ by the empirical correlations their optimized values were employed. The correlations of $D_{ax,L}$ and $(Ka)_{LS}$ like function of the volumetric flow rate of the liquid phase.*

Keywords*: Experimental procedure, NaOH tracer, TBRs, Gas-Liquid-Solid System, dynamic modelling*

1. INTRODUCTION

Trickle-bed reactors (TBRs) can be defined as fixed beds of catalyst particles in contacted with the cocurrent downward flows of gas and liquid phases at low superficial velocities. These reactors assume greater importance among the there-phase gas-liquid-solid reaction systems encountered in industrial processes. TBRs are extensively used in many process industries. These reactors are widely employed in petroleum refineries for hydrotreating, hydrodemetalization, and hydrocracking applications. On the other hand, they also are widely used for carrying out a variety of processes such as petrochemical, chemical, biochemical, and waste treatment. There are many works in the literature to model and describe the behaviour of processes of those TBRs. The behaviour to many of those works can be studied applying mathematical modelling.

Mathematical models of TBRs represent an ancillary tool for minimizing the experimental efforts required to developing this important equipment in industrial plants. Experiment and prototype development are the main requirements for accurate engineering design in any industrial process. However, mathematical modelling and numerical simulation are in continuous development, contributing in a growing form for the better understanding of processes and physical phenomena, and thereby for design. Besides, mathematical models require experiment in order to be validated and the required experiments involve complex measurements of difficult accomplishment. Therefore, mathematical modelling also represents an incentive for the development of new experimental methods and techniques.

There are various mathematical models of completely or partially wetted catalyst particles which may exist in TBRs. Each of those models is based on many assumptions and is forced to use simplifications in order to solve the complex equation systems. Normally, mathematical models of TBRs may involve the mechanisms of forced convection, axial dispersion, interphase heat and mass transfers, intraparticle diffusion, adsorption, and chemical reaction (Silva et al., 2003; Burghardt et al., 1995; Iliuta et al., 2002; Latifi et al., 1997).

Various flow regimes exist in a TBR depending on the liquid and gas mass flow rates, the properties of the fluids and the geometrical characteristics of the packed bed (Charpentier and Favier, 1975). A fundamental understanding of the hydrodynamics of TBRs is indispensable in their design, scale-up, and performance. The hydrodynamics are affected differently in each flow regime. The basic hydrodynamics parameters for the design, scale-up and operation are the pressure gradient and liquid saturation. The pressure gradient is related to the mechanical energy dissipation due to the two-phase flow through the fixed bed of solid particles. The liquid saturation, which partially occupies the void volume of the packed bed, is related to other important hydrodynamics parameters as the pressure gradient, the external wetting of the catalyst particles, the mean residence time of the liquid phase in the reactor and the heat and mass transfer phenomena (Specchia and Baldi, 1977).

The objective of the work is to estimate and describe the behaviour of the axial dispersion coefficient of the liquid phase, $D_{ax,L}$, and overall liquid-solid mass transfer, $(Ka)_{LS}$, coefficient using a set of experiments carried out in a laboratory scale TBR. Comparing the mathematical model with experimental data. Analyzing the correlations from the $D_{ax,L}$ and $(Ka)_{LS}$ as a function of the volumetric flow rate

2. MATHEMATICAL MODEL

To model the mathematical modelling according to the liquid-solid model, in which the liquid phase (H_2O + NaOH tracer) was deal as a continuum in a fixed bed of solid particles. An one-dimensional mathematical model was adopted in which the axial dispersion, liquid-solid mass transfer, partial wetting and reaction phenomena are present. This model has been used for the liquid phase by using the NaOH as tracer and is restricted to the following assumptions: (i) isothermal system; (ii) all flow rates are constant throughout the reactor; (iii) the intraparticle diffusion resistance has been neglected; (iv) in any position of the reactor the chemical reaction rate within the solid is equal to the liquid-solid mass transfer rate.

- mass balance for the liquid;

$$h_L \frac{\partial C_L(z,t)}{\partial t} + \frac{4Q_L}{\pi d_r^2}\frac{\partial C_L(z,t)}{\partial z} = D_{ax,L}\frac{\partial^2 C_L(z,t)}{\partial z^2} - (1-\varepsilon_s)\ \mathrm{PWE}\ (Ka)_{LS}[C_L(z,t) - C_S(z,t)] \tag{1}$$

- The initial and boundary conditions for Eq. (1) are:

$$C_L(z,0) = C_{L,0} \tag{2}$$

$$D_{ax,L}\frac{\partial C_L(z,t)}{\partial z}\bigg|_{z=0^+} = \frac{4Q_L}{\pi d_r^2}\Big[C_L(z,t)\big|_{z=0^+} - C_L(z,0)\Big] \tag{3}$$

$$\frac{\partial C_L(z,t)}{\partial z}\bigg|_{z=L} = 0 \tag{4}$$

- Combining the chemical reaction rate with the mass transfer rate:

$$(Ka)_{LS}[C_L(z,t) - C_S(z,t)] = k_r\, C_S(z,t)\eta\varepsilon_S \tag{5}$$

Eqs (1) to (5) can be analyzed with dimensionless variable terms, see Table (1):

Table-1: Summary of dimensionless variables

liquid and solid concentrations, dimensionless	Time and coordinate axial direction, dimensionless
$\Gamma_L(\xi,\tau) = \frac{C_L(z,t)}{C_{L,0}}$	$\tau = \frac{4\,Q_L\,t}{L\,h_L\,\pi\,d_r^2}$
$\Gamma_S(\xi,\tau) = \frac{C_S(z,t)}{C_{L,0}}$	$\xi = \frac{z}{L}$

Writing Eqs. (1) to (5) in dimensionless forms:

$$\frac{\partial \Gamma_L(\xi,\tau)}{\partial \tau} + \frac{\partial \Gamma_L(\xi,\tau)}{\partial \xi} = \frac{1}{P_E}\frac{\partial^2 \Gamma_L(\xi,\tau)}{\partial \xi^2} - \alpha_{LS}[\Gamma_L(\xi,\tau) - \Gamma_S(\xi,\tau)] \tag{6}$$

$$\Gamma_L(\xi,0) = 1 \tag{7}$$

$$\frac{\partial \Gamma_L(\xi,\tau)}{\partial \xi}\bigg|_{\xi=0^+} = P_E\Big[\,\Gamma_L(\xi,\tau)\big|_{\xi=0^+} - 1\,\Big] \tag{8}$$

$$\frac{\partial \Gamma_L(\xi,\tau)}{\partial \xi}\bigg|_{\xi=1} = 0 \tag{9}$$

$$\Gamma_L(\xi,\tau) - \Gamma_S(\xi,\tau) = \beta_S\ \Gamma_S(\xi,\tau) \tag{10}$$

Eqs. (6) through (10) include the following dimensionless parameters:

$$\alpha_{LS} = \frac{(1-\varepsilon_s)\,F_M\,(Ka)_{LS}\,L\,\pi\,d_r^2}{4Q_L} \tag{11}$$

$$P_E = \frac{4\, Q_L\, L}{D_{ax,L}\, \pi\, d_r^2} \tag{12}$$

$$\beta_S = \frac{k_r\, \eta\, \varepsilon_s}{(Ka)_{LS}} \tag{13}$$

2. ANALYTICAL SOLUTION

The solution of transport problems in three-phase systems is very complex and usually numerical approximation methods are used. On the other hand, analytical solutions are used for the simple models. Although the analytical solutions are simple, the boundary conditions proposed for these models need a careful attention. The majority of the analytical solutions belong to infinite and semi-infinite field. The analytical solutions for the finite field have been developed by Feike and Torid (1998) and Dudukovic (1982). In these works, the authors adopt the analytical procedure in the finite field region ($0 \le z \le L \rightarrow 0 \le \xi \le 1$) where the method of separation of variables is used. The $\Gamma_S(\xi, \tau)$ was isolated from Eq. (10) and it was introduced in Eq. (6), reducing it to:

$$\frac{\partial \Gamma_L(\xi,\tau)}{\partial \tau} + \frac{\partial \Gamma_L(\xi,\tau)}{\partial \xi} = \frac{1}{P_E} \frac{\partial^2 \Gamma_L(\xi,\tau)}{\partial \xi^2} - \gamma\, \Gamma_L(\xi,\tau) \tag{14}$$

where:

$$\gamma = \frac{\alpha_{LS}\, \beta_S}{\beta_S + 1} \tag{15}$$

The analytical solution of Eq. (14) was obtained by the separation of variables method using the following relation:

$$\Gamma_L(\xi,\tau) = N_L(\xi) * Z_L(\tau) \tag{16}$$

Then, Eq. (14) was separated in two ordinary differential equations with constant coefficients:

$$\frac{d\, Z_L(\tau)}{d\, t_d} + \lambda^2\, Z_L(\tau) = 0 \tag{17}$$

$$\frac{d^2 N_L(\xi)}{d\xi^2} - \frac{d\, N_L(\xi)}{d\xi} + \left(\lambda^2 - \gamma\right) P_E\, N_L(\xi) = 0 \tag{18}$$

The global solution of Eqs. (17) and (18) for $\xi = 1$ is given by:

$$\Gamma_L(\tau) = \sum_{n=0}^{\infty} \frac{1.6}{T_{2,n}(\lambda_n)\, T_{3,n}(\lambda_n) - T_{1,n}(\lambda_n) T_{4,n}(\lambda_n)} \left\{ \left[T_{2,n}(\lambda_n) - T_{3,n}(\lambda_n) \sin\varphi_n(\lambda_n) \cos\varphi_n(\lambda_n) \right] + \right.$$
$$\left. T_{4,n}(\lambda_n) \cos\varphi_n(\lambda_n) \left[\cos\varphi_n(\lambda_n) - 1\right] + \sin\varphi_n(\lambda_n) \left[T_{3,n}(\lambda_n) - T_{1,n}(\lambda_n) \sin\varphi_n(\lambda_n) \right] \right\} e^{-\lambda_n^2 \tau} \tag{19}$$

Where,

$$T_{1,n}(\lambda_n) = \frac{1}{1 + 16\, [\varphi_n(\lambda_n)]^2} \left\{ \varphi_n(\lambda_n) \left[3.2 \sin\varphi_n(\lambda_n) \cos\varphi_n(\lambda_n) + 0.6\, \varphi_n(\lambda_n) \right] + \sin^2 \varphi_n(\lambda_n) \right.$$
$$\left. \left[0.8 + 25.6 [\varphi_n(\lambda_n)]^2 \right] \right\} \tag{20}$$

$$T_{2,n}(\lambda_n) = \frac{\varphi_n(\lambda_n)}{1 + 16\, [\varphi_n(\lambda_n)]^2} \left\{ 3.3 \sin^2 \varphi_n(\lambda_n) - 13.2 \sin\varphi_n(\lambda_n) \cos\varphi_n(\lambda_n) + 0.4 [\varphi_n(\lambda_n)] \right\} \tag{21}$$

$$T_{3,n}(\lambda_n) = \frac{1}{1 + 16 [\varphi_n(\lambda_n)]^2} \left\{ 3.3\, \varphi_n(\lambda_n) \cos^2 \varphi_n(\lambda_n) + 13.2\, [\varphi_n(\lambda_n)]^2 + \cos\varphi_n(\lambda_n) \sin\varphi_n(\lambda_n) - 2 \right.$$
$$\left. \varphi_n(\lambda_n) - 10.4\, [\varphi_n(\lambda_n)]^3 \right\} \tag{22}$$

$$T_{4,n}(\lambda_n) = \frac{1}{1 + 16\, [\varphi_n(\lambda_n)]^2} \left\{ 1.6 \sin^2 \varphi_n(\lambda_n) \left\{ 1 + 16\, [\varphi_n(\lambda_n)]^2 \right\} + 3.2\, \varphi_n(\lambda_n) \cos\varphi_n(\lambda_n) \right.$$
$$\left. \sin\varphi_n(\lambda_n) - 10.4\, [\varphi_n(\lambda_n)]^3 \right\} \tag{23}$$

$$\varphi_n(\lambda_n) = \frac{1}{2} \left\{ 4 P_E \left\{ \left[\left(2n + \tfrac{1}{2}\right)\pi \right]^2 - \gamma \right\} - 1 \right\}^{1/2}; \quad \lambda_n = (2\, n + ½); \; (n = 0, 1, 2, 3, \ldots) \tag{24}$$

4. MATERIALS AND METHODS

The experiments were realized in a three-phase trickle bed reactor, which consists of a fixed bed with a height of 0.22 m and an inner diameter of 0.030 m with catalytic particles contacted by a cocurrent gas-liquid downward flow carrying the liquid tracer in the liquid phase. The experiments have been performed at conditions where the volumetric flow rates of the gas and liquid phases were maintained at such a level to guarantee a low interaction regime with Q_L in the range of 7.068 x 10^{-8} m^3 s^{-1} to 2.122 x 10^{-6} m^3 s^{-1} and Q_G in the range of 1.414 x 10^{-5} m^3 s^{-1} to 3.181 x 10^{-4} m^3 s^{-1} in pilot plant trickle be reactors (Ramachandran and Chaudhari, 1983).
Continuous analysis of the NaOH tracer, at a concentration of 10 mol m^{-3}, were made using HPLC/UV-CG 480C at the outlet of the fixed bed. Results have been expressed in term of the tracer concentrations versus time.
The methodologies applied to evaluating the axial dispersion of the liquid phase and overall liquid-solid mass transfer effects for the (N_2/H_2O-NaOH/activated carbon) system were:

- comparison of the experimental results with the Eq. (28) developed for the system;
- evaluation of the $D_{ax,L}$ and $(Ka)_{LS}$ parameters of the mathematical model, in which the initial values are obtained from the correlations in Table (2);
- optimization of the $D_{ax,L}$ and $(Ka)_{LS}$ parameters by the comparison between the experimental and calculated data by the Eq. (25).

The axial dispersion coefficient of the liquid phase and overall liquid - solid mass transfer coefficient have been determined simultaneously by the comparison between the experimental and theoretical data, obtained at the outlet of the fixed bed, subject to the minimization of the objective function (F), given by:

$$F\left[D_{ax,L},(Ka)_{LS}\right]=\sum_{k=1}^{N}\left\{\left[\Gamma_L(\tau)\right]_k^{Exp}-\left[\Gamma_L(\tau)\right]_k^{Eq.(19)}\right\}^2 \tag{25}$$

5. RESULTS AND DISCUSSIONS

The experimental results of the tracer in a laboratory scale TBR have been performed in twenty runs varying the volumetric flow rate (Q_L) of the liquid phase. Experimental procedures and results are presented and discussed in detail in the trickling flow regime. Results obtained by the mathematical model have been compared with both sets of experiments. An objective function (F) has been calculated and presented. Values of this objective function indicate a very good agreement between the mathematical model and both types of experiments. The computation methodology to optimize the axial dispersion coefficient ($D_{ax,L}$) of the liquid phase and overall liquid-solid mass transfer $(Ka)_{LS}$ coefficients has to use an optimization subroutine with minimization of the objective function (Box, 1965).

Table -2: Correlations for the obtainment of the D_{ax}, k_{LS} and PWE, the initial values

Correlations	References
$D_{ax,L}=0.55\left(Re_L\right)^{0.61}$ (26)	Lange et al. (1999)
$(Ka)_{LS}=2.514\dfrac{\left[1-\left(h_L/\varepsilon_{ex}\right)\right]D_L}{d_p^2}\left(R_L\right)^{0.73}\left(R_G\right)^{0.2}\left(Sc_L\right)^{0.5}\left(\dfrac{d_p}{d_r}\right)^{0.2}$ (27)	Fukushima and Kusaka, (1977)
$PWE=3.40\left(Re_L\right)^{0.22}\left(Re_G\right)^{-0.08}\left(Ga_L\right)^{-0.51}$ (28)	Burghardt et al. (1990)

The calculating of the NaOH concentrations from the mathematical model, for the system N_2/H_2O - NaOH / activated carbon, includes various fixed parameters. The values of the fixed parameters used in the parameter-fitting calculations are given in Table (3).

The $D_{ax,L}$ and $(Ka)_{LS}$ have been optimized from different volumetric flow rate of the liquid phase and it changes from 4.248 x 10^{-6} to 5.581 x 10^{-7} m^3 s^{-1}. The $D_{ax,L}$ of the liquid phase was varying from 3.186 x 10^{-5} to 0.735 x 10^{-5} m^2 s^{-1} using H_2O and NaOH as liquid fluids. On the other hand, the $(Ka)_{LS}$ also was changing from 2.496 x 10^{-2} to 0.124x10^{-2} s^{-1}. The range objective function range has been, respectively, from 1.572 x 10^{-4} to 1.212 x 10^{-4}. The optimization of the $D_{ax,L}$ and $(Ka)_{LS}$ for all twenty runs has been performed with the minimization of the objective function, Eq. (25). Values of the $D_{ax,L}$ and $(Ka)_{LS}$ for all twenty runs differ in order of magnitude.

The tracer method has been developed in our laboratory to evaluate the external fluid-solid contacting efficiency because it produces rapidly contacting information (Silva et al., 2003). Therefore, the objective of the present work has been an experimental and theoretical investigation with the tracer introduced in liquid stream. First, experimentally obtained tracer concentrations have to be unified with the tracer answers obtained by the mathematical model. In experiments, the concentrations of the tracer have been determined in the time domain using HPLC/UV-CG480C at the outlet of the fixed bed TBR. The dimensionless dynamic concentration profiles are shown in Figs. (1a) and (1b). The agreement of these Figs. has been very well satisfactory especially between theoretical and experimental results. Figs.

(1a) and (1b) have been obtained in different volumetric flow rate. These Figs. show clearly the validation of the mathematical model, Eq. (19), with physical reality.

Table - 3: Summary of intervals of operating conditions for the particle-fluid (Colombo et al., 1976 and Silva et al., 2003)

Category	Properties	Numerical Values
Operating Conditions	Pressure (P), atm	1.01
	Temperature (T), K	298.00
	Volumetric flow rates of the liquid phase $(Q_L)x10^6$, $m^3\ s^{-1}$	4.248-0.558
	Volumetric flow rates of the gas phase $(Q_G)x10^5$, $m^3\ s^{-1}$	9.861
	Standard acceleration of gravity (g), $m\ s^{-2}$	9.81
Packing and bed properties	Total bed height $(L)x10^2$, m	0.22
	Bed porosity (ε_s)	0.59
	External porosity (ε_{ex})	0.39
	Effective liquid-solid mass transfer area per unit column Diameter of the catalyst particle $(d_p)x10^4$, m	3.90
	Diameter of the reactor $(d_r)x10^2$, m	3.00
	Density of the particle $(\rho_p)x10^{-3}$, $kg\ m^{-3}$	2.56
	reaction rate constant $(k_r)x10^{-1}$, $kgmol\ kg^{-1}\ s^{-1}$	5.41
Liquid properties	Density of the liquid phase $(\rho_l)x10^{-3}$, $kg\ m^{-3}$	1.01
	Liquid molecular diffusivity $(D_L)x10^{10}$, $m^2\ s^{-1}$	5.81
	Viscosity of the liquid phase $(\mu_l)x10^{-4}$, $kg\ m^{-1}\ s^{-1}$	8.96
	Surface tension $(\sigma_l)x10^2$, $N\ m^{-1}$	5.51
	Dynamic liquid holdup $(h_L)x10^1$	4.91
Gas properties	Density of the gaseous phase $(\rho_g)x10^1$, $kg\ m^{-3}$	6.63
	Viscosity of the gaseous phase $(\mu_g)x10^5$, $kg\ m^{-1}\ s^{-1}$	1.23

In Fig. (1a), the fitted curve according to the experimental model has been compared to a transient mathematical model simulation for a volumetric flow rate from $3.751x10^{-5}$ $m^2\ s^{-1}$. The axial dispersion coefficient of the liquid phase for this experiment was from $2.836x10^{-5}$ $m^2\ s^{-1}$. The overall liquid-solid mass transfer coefficient for this run was from $2.196x10^{-2}$ s^{-1}. The Peclet number for this experiment was from 149.692. The objective function for this experiment was from $1.423x10^{-4}$. It can be noticed that the computer time has been from 9s in the simulation. The saturation exhibits a propagation front experimental and theoretical behaviour around $\tau = 190$, hence showing that the mathematical model of this work has been correctly presented.

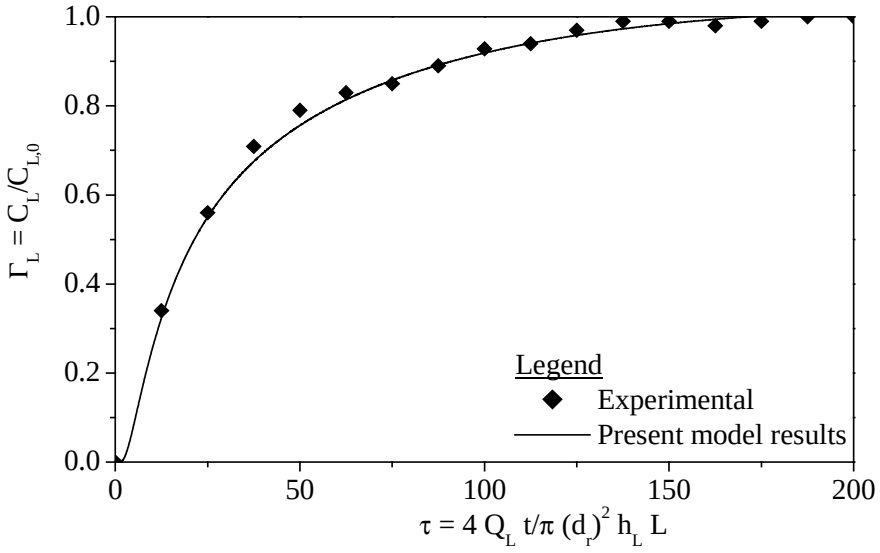

(a)

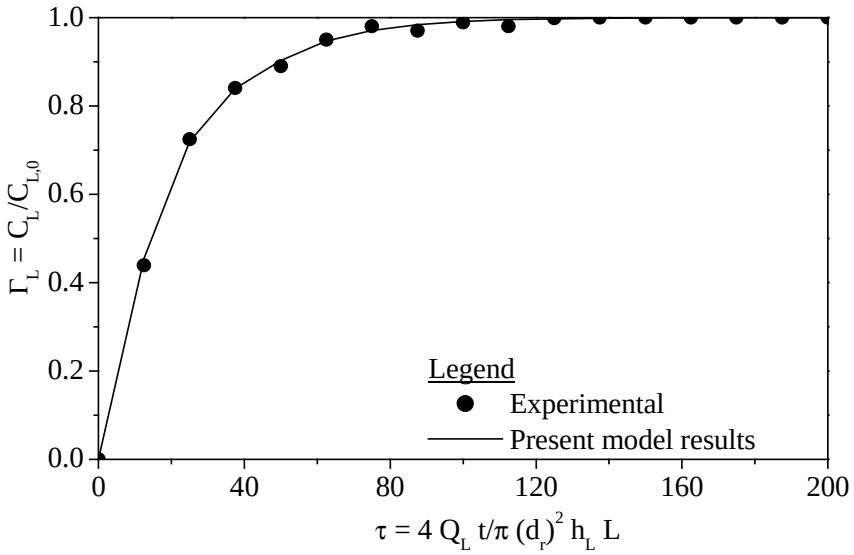

(b)

Figure 1: Concentration profiles of the NaOH tracer at the outlet of the N_2/H_2O-NaOH/activated carbon in operating conditions from $4.248x10^{-6} \leq Q_L \leq 5.581x10^{-7} m^3\ s^{-1}$; $Q_G = 9.861x10^{-5}\ m^3\ s^{-1}$

In Fig. (1b), the fitted curve according to the experimental model also has been compared to a transient mathematical model simulation for a volumetric flow rate from $1.096x10^{-6}\ m^3\ s^{-1}$. The axial dispersion coefficient of the liquid phase for this run was from $1.105x10^{-5}\ m^2\ s^{-1}$. The overall liquid-solid mass transfer coefficient for this experiment was from $0.975x10^{-2}\ s^{-1}$. The objective function for this run was from $1.015x10^{-4}$. The Peclet number for this run has been from 112.256. It can be observed that the computer time was 6s in simulation. The saturation shows a propagation front experimental and theoretical behaviour around $\tau = 120$, hence showing that the mathematical model of this work was correctly presented.

Analysis of the axial dispersion coefficient of the liquid phase and overall liquid-solid mass transfer coefficient in the concurrent gas-liquid trickle bed reactors has mostly been performed with empirical correlations in a specific range of operating conditions. The axial dispersion coefficient was calculated in terms of the volumetric flow rate of the liquid phase as well as the overall liquid-solid mass coefficient also has been computed in functions of the same volumetric flow rate of the liquid phase. It can be observed that the axial dispersion coefficient, $D_{ax,L}$, of the liquid phase and overall liquid-solid mass transfer coefficient, $(Ka)_{LS}$, increase with an increase in volumetric flow rate.

In the studied trickling flow regime, our experimental results for the axial dispersion coefficient of the liquid phase as well as the overall liquid-solid mass coefficient are well correlated by means of the following equations:

$$D_{ax,L} = 88.149(Q_L)^{1.248},\ R^2 = 0.9967;\ 4.248x10^{-6} \leq Q_L \leq 5.581x10^{-7} m^3\ s^{-1};\ Q_G = 9.861x10^{-5}\ m^3\ s^{-1} \quad (29)$$

$$(Ka)_{LS} = 40.791(Q_L)^{2.127}\ R^2 = 0.9978;\ 4.248x10^{-6} \leq Q_L \leq 5.581x10^{-7} m^3\ s^{-1};\ Q_G = 9.861x10^{-5}\ m^3\ s^{-1} \quad (30)$$

The exponent and pre-volumetric flow rate term of Eqs. (29) and (30) were optimized. The accuracy of these four parameters have been very satisfactory, particularly, the exponent of the volumetric flow rate. It can be seen in Table (4) the parameters with their accuracies.

Table - 4: Confidence intervals from 95%

Equation (29)		Equation (30)	
Parameters	Accuracy (%)	Parameters	Accuracy (%)
88.149	9.16	40.791	10.32
1.248	3.78	2.127	4.13

The mean relative error between the predicted and experimental values from $D_{ax,L}$ and $(Ka)_{LS}$ are computed from:

$$\left\langle \varphi_{D_{ax,L}} \right\rangle = \frac{1}{n} \sum_{i=1}^{m} \frac{\left| D_{ax,L}^{Pred.} - D_{ax,L}^{Exp.} \right|}{D_{ax,L}^{Exp.}} \tag{31}$$

$$\left\langle \varphi_{(Ka)_{LS}} \right\rangle = \frac{1}{n} \sum_{i=1}^{m} \frac{\left| (Ka)_{LS}^{Pred.} - (Ka)_{LS}^{Exp.} \right|}{(Ka)_{LS}^{Exp.}} \tag{32}$$

$\langle D_{ax,L} \rangle$ and $\langle (Ka)_{LS} \rangle$ are analyzed from the mean quadratic deviation defined as the square root of the quadratic variance.

$$\sigma_{D_{ax,L}} = \left\{ \sum_{k=1}^{m} \frac{\left[\left\langle D_{ax,L} \right\rangle - D_{ax,L} \right]^2}{n} \right\}^{1/2} \tag{33}$$

$$\sigma_{(Ka)_{LS}} = \left\{ \sum_{k=1}^{m} \frac{\left[\left\langle (Ka)_{LS} \right\rangle - (Ka)_{LS} \right]^2}{n} \right\}^{1/2} \tag{34}$$

Fig (2) shows the variations of experimental results of the axial dispersion coefficient of the liquid phase and theoretical predictions computed from the Eq. (29) as function of the volumetric flow rate. It can be known that the agreement between theoretical and experimental values of the axial coefficient of the liquid phase is satisfactory, especially at all range of the volumetric flow rate. The mean relative error $\langle \varphi_{Dax,L} \rangle$ between the predicted and experimental results of this hydrodynamic parameter has been calculated by the Eq. (31). On the other hand, the deviation of the relative error around the mean value $\langle \sigma_{Dax,L} \rangle$ was quantified from the Eq. (33). The results of the mean relative error and quadratic deviation were obtained for twenty runs, respectively, from $\langle \varphi_{Dax,L} \rangle$ = 8.57% and $\langle \sigma_{Dax,L} \rangle$ = 6.21%.

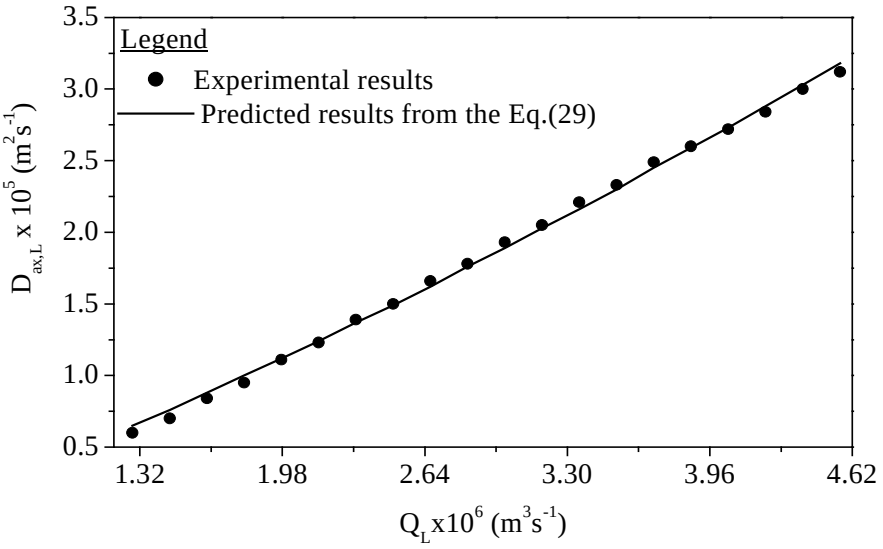

Figure-2: Axial Dispersion Coefficient of the Liquid Phase as a Function of the Volumetric Flow Rate

Fig (3) presents the changes of experimental data of the overall liquid-solid mass transfer coefficient and theoretical predictions obtained from the Eq. (30). It can be seen that the comparison between theoretical and experimental results overall liquid-solid mass transfer coefficient is very satisfactory, especially at all variations of the volumetric flow rate. The mean relative error $\langle \varphi_{(Ka)LS} \rangle$ between the predicted and experimental values of this parameter has been computed by

the Eq. (32). Furthermore, the deviation of the relative error around the value $\langle\sigma_{(Ka)LS}\rangle$ be seen calculated from the Eq. (34). The values of the mean relative error and quadratic deviation have been estimated for twenty experiments, respectively, from $\langle\varphi_{(Ka)LS}\rangle$ = 9.71% and $\langle\sigma_{(Ka)LS}\rangle$ = 6.83%.

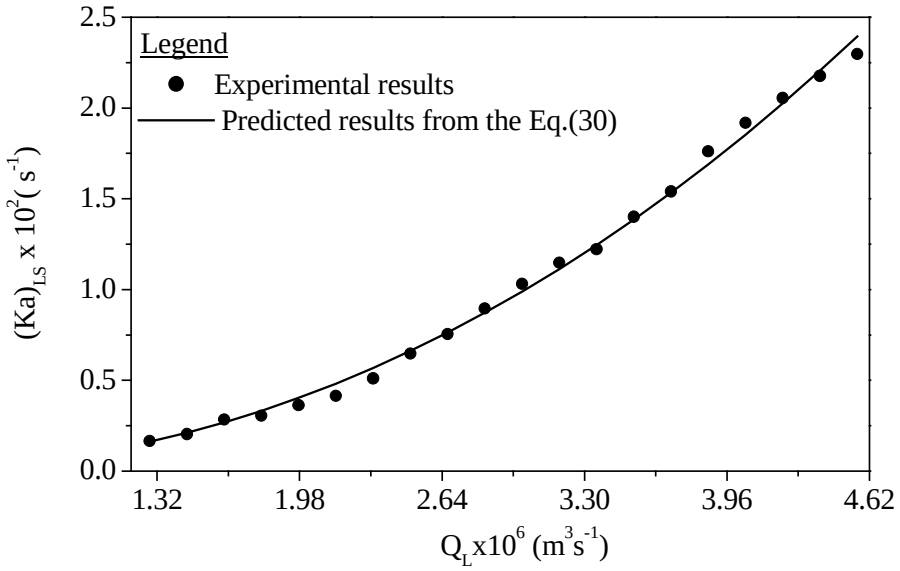

Figure-3: Overall Liquid-Solid mass Transfer Coefficient as a Function of the Volumetric Flow Rate

6. CONCLUSIONS

The objective of this paper has been to realize an analysis of the axial dispersion coefficient of the liquid phase and overall liquid-solid mass transfer coefficient using the NaOH tracer in a TBR under trickling flow conditions. In a first step, it has been shown the analytical solution of the mathematical model developed for the NaOH tracer in the TBR. In a second step, it has been optimized the $D_{ax,L}$ and $(Ka)_{LS}$ simultaneously by the comparison between experimental results and the Eq. (19) through the Eq. (25). In a third step, it has been validated on the basis of a comparison between the experimental results and theoretical predictions obtained from the Eq (19) according to Figs. (1a) and (1b). In a fourth step, it has been proposed the correlations for the axial dispersion coefficient of the liquid phase and overall liquid-solid mass transfer coefficient as a function from the volumetric flow rate according to Eqs. (29) and (30). In a fifth step, it has been shown the behaviour for the axial dispersion coefficient of the liquid phase and overall liquid-solid mass transfer coefficient as a function from the volumetric flow rate according to the Figs. (2) and (3). Furthermore, the statistical analysis through confidence intervals showed that all the parameters involved in the correlations from the $D_{ax,L}$ and $(Ka)_{LS}$ were estimated very accurately.

ACKNOWLEDGMENTS

The author would like to thank CNPq (Conselho nacional de Desenvolvimento e Tecnológico) for financial support (process 483541/07-9).

NOMENCLATURE

$C_L(z,t)$	Concentration of the liquid tracer in the liquid phase, kg m^{-3}
$C_S(z,t)$	Concentration of the liquid tracer in the external surface of solid, kg m^{-3}
$D_{ax,L}$	Axial dispersion coefficient for the liquid tracer in the liquid phase, m^2 s^{-1}
D_L	Liquid molecular diffusivity, m^2 s^{-1}
d_P	Diameter of the catalyst particle, m
d_r	Diameter of the reactor, m
F	Objective function
PWE	wetting factor, dimensionless
Ga_L	Galileo number, $G_{a_L} = d_p^3 g \rho_L^2 / \mu_L$
h_L	Dynamic liquid holdup, dimensionless

i Complex number $\sqrt{-1}$
$(Ka)_{LS}$ overall liquid-solid mass transfer coefficient, s^{-1}
k_r Reaction constant, kgmol kg^{-1} s^{-1}
L Height of the catalyst bed, m
$N_L(\xi)$ Defined function in Eq. (16)
P_E Peclet number, $P_E = V_{SL} L / D_{ax}$
Q_L Volumetric flow rates of the liquid phase, m^3 s^{-1}
Q_G Volumetric flow rates of the gas phase, m^3 s^{-1}
Re_L Reynolds number, $Re_L = V_{SL} \rho_L d_r / \mu_L$
Re_G Reynolds number, $Re_G = V_{SG} \rho_G d_r / \mu_G$
Sc_L Schmidt number, $Sc_L = \mu_L / \rho_L D_L$
t Time, s
z Axial distance of the catalytic reactor, m
$Z_L(\tau)$ Function defined in Eq. (16)

Greek Letters

α_{LS} Parameter defined in Eq. (11), dimensionless
β_S Parameter defined in Eq. (13), dimensionless
ε_{ex} External porosity, dimensionless
ε_S Bed porosity, dimensionless
$\Psi_i(\xi,\tau)$ Dimensionless concentration of the tracer in liquid and solid, i = L, S
η Catalytic effectiveness factor
μ_L Viscosity of the liquid phase, kg m^{-1} s^{-1}
ξ Parameter defined in Table 1, dimensionless
ρ_L Density of the liquid phase, kg m^{-3}

REFERENCES

Box, P., 1965, “A new method of constrained optimization and a comparison with other method”, Computer Journal, Vol. 8, pp. 42-52.

Burghardt A., Bartelmus G., Jaroszynski M., Kolodziej A., 1995, “Hydrodynamics and mass transfer in a three-phase fixed bed reactor with concurrent gas-liquid downflow”, Chemical Engineering and Processing, Vol. 28, pp. 83-99.

Burghardt A., Kolodziej, A. S., Jaroszynski M., 1990, “Experimental studies of liquid-solid wetting efficiency in trickle-bed cocurrent reactors”, Chemical Engineering Journal, Vol. 28, pp. 35-49.

Charpentier, J. C.; Favier, M., 1975. Some liquid holdup experimental data in trickle bed reactors for foaming and non foaming hydrocarbons, Aiche Journal, 21, 1213-1221.

Dudukovic M. P., 1982, “Analytical solution for the transient response in a diffusion cell of the wickle- kallenbach type”, Chemical Engineering Science, Vol. 37, pp. 153-158.

Feike J. L., Toride N., 1998, “Analytical solutions for solute transport with binary and ternary exchange”, Soil Sci. Soc. Am. J, Vol. 56, pp. 855-864.

Fukushima, S., Kusaka, K., 1977, “Interfacial area boundary of hydrodynamic flow region in packed column with cocurrent downward flow, Journal of Chemical Engineering of Japan, Vol. 10, No. 6, pp. 461-467.

Iliuta, I, Bildea, S. C., Iliuta, M. C., Larachi, F., 2002, “Analysis of trickle-bed and packed bubble column bioreactors for combined carbon oxidation and nitrification”, Brazilian Journal of Chemical Engineering, Vol. 19, pp. 69-87.

Lange, R., Gutsche, R., Hanika, J., 1999, “Forced periodic operation of a trickle-bed reactor”, Chemical Engineering Science, Vol. 54, pp. 2569-2573.

Latifi, M. A., Naderifar, A., Midoux, N., 1997, “Experimental investigation of the liquid-solid mass transfer at the wall of trickle-bed - Influence of Schmidt Number”, Chemical Engineering Science, Vol. 52, pp. 4005- 4011.

Liu, G., Zhang, X., Wang, L., Zhang, S., Mi, Z., 2008, “Unsteady-state operation of trickle-bed reactor for dicyclopentadiene hydrogenation”, Chemical Engineering Science, Vol. 36, pp. 4991-5001.

Ramachandran P. A., Chaudhari, R. B., 1983, “Three phase catalytic reactors”, Gordan and Breach Science Publishers, New York, U.S.A., Chap. 7, pp. 200-255.

Silva, J. D., Lima, F. R. A.; Abreu, C. A. M.; Knoechelmann, A, 2003, “Experimental analysis and evaluation of the mass transfer process in a trickle bed regime”, Brazilian Journal of Chemical Engineering, Vol. 20, No.4, pp. 375-390.

Specchia, V. and Baldi, G., Pressure Drop and Liquid Holdup for Two Phase Concurrent Flow in Packed Beds, Chem. Eng. Sci, 32, 515-523 (1977).